

Channel-Aware Spectrum Sensing and Access for Mobile Cognitive Radio Ad Hoc Networks

Yuan Lu, Alexandra Duel-Hallen, *Fellow, IEEE*

Abstract—In hardware-constrained cognitive radio (CR) ad hoc networks, secondary users (SUs) with limited sensing capabilities strive to discover and share available spectrum resources without impairing primary user (PU) transmission. Sensing strategy design objectives include high CR network throughput, resolved SU competition, distributed implementation, and reliable performance under node mobility. However, these objectives have not been realized by previously investigated sensing strategies. A novel sensing strategy is analyzed where the reward is adapted to the SU link channel state information (CSI) prior to sensing, thus randomizing sensing decisions and boosting the network throughput. Moreover, CSI-aided sensing is combined with a novel first-come-first-served (FCFS) medium access control (MAC) scheme that resolves SU competition prior to sensing. Finally, a pilot-based CSI prediction method is developed to enable the proposed CSI-aided sensing strategies for mobile scenarios. Analytical and numerical results demonstrate that the proposed sensing and access methods significantly outperform nonadaptive sensing strategies for practical mobile CR scenarios with CSI mismatch and pilot overhead.

Index Terms—Ad hoc network, channel state information (CSI), cognitive radio (CR), medium access control (MAC), sensing strategy.

I. INTRODUCTION

COGNITIVE radio (CR) can potentially aid utilization of hidden spectrum opportunities while limiting disruption to licensed, or primary users (PUs) and without changing the existing communication infrastructure of the primary network. In a CR network, unlicensed, or secondary users (SUs) sense PU channels to identify spectrum holes. However, SUs' sensing capabilities are usually limited in software-defined radio (SDR) systems due to hardware limitations [2]. Moreover, it is often necessary to make autonomous sensing decisions without the coordination of a central controller [3]. This paper focuses on distributed sensing strategy design for multiple SUs and multiple channels under hardware constraints.

Resolving congestion among SUs is challenging in hardware-constrained autonomous CR networks. Traditionally, sensing decisions are made using channel availability information, e.g., a statistical model of PU traffic [4]. For example, the myopic sensing policy [5] bases sensing choices exclusively on PU occupancy. However, since the PU transmission range is typically larger than the SU range [3] as illustrated in Fig. 1, all neighboring SUs make similar sensing decisions when the myopic strategy is employed, leading to potential SU collisions

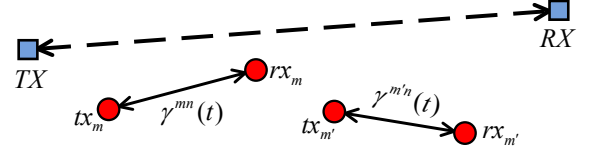


Fig. 1. A PU TX-RX pair and SU tx-rx pairs m and m' .

[6]. In principle, fair medium access for each idle channel can be accomplished using carrier sensing, random backoff, control message exchange, etc., so the SUs competing for the same channel are equally likely to gain access, and SU collisions at the physical layer are avoided. However, in a hardware-constrained CR network, a collision-avoidance medium access control (MAC) scheme alone is not sufficient since it results in poor spectrum utilization and low CR network throughput. To improve the throughput, a randomized sensing policy which spreads SUs' sensing decisions over different channels is necessary. Several strategies in the literature, e.g., [4], [6]–[10], address this issue by randomizing sensing decisions, using negotiation, or employing game theory, but these strategies provide limited throughput improvement because they reduce an SU's ability to sense its preferred channel.

One limitation of previously proposed sensing strategies is the choice of reward given by the channel bandwidth, which does not diversify sensing choices. In [1], we have proposed to *adapt the reward to the instantaneous channel gain of the SU transmitter-receiver link*. This reward varies over SU locations and frequencies due to channel fading and thus randomizes sensing decisions. Moreover, SUs boost their individual throughputs by favoring spectrum opportunities with high expected transmission rates.

The proposed strategy matches the reward employed by the SUs to the data rate achieved during transmission. We assume that the SU transmitter obtains the channel state information (CSI) and adapts to it. Adaptation to the CSI of the secondary link to improve channel access and/or transmission rate has been proposed in, e.g., [11]–[13]. However, in these references, adaptation took place after sensing and thus did not help to alleviate SU congestion when making sensing decisions. To the best of our knowledge, adaptation to SU link CSI prior to sensing was explored only in [14]–[16]. However, in [14] and [15], SUs sense multiple channels prior to transmission while our work focuses on one-shot sensing to reduce the sensing load. Moreover, collision resolution requires excessive message exchange on the control channel in [15] and is not included in [14], [16]. In contrast, we propose to combine CSI-aided sensing with novel first-come-first-served (FCFS) MAC and demonstrate throughput advantages of this combination as

This research was supported by the NSF grant CNS-1018447. This paper was presented in part at the IEEE Consumer Communications and Networking Conference, Las Vegas, NV, Jan. 2013 [1].

The authors are with the Department of Electrical and Computer Engineering, North Carolina State University, Raleigh, NC, 27606 USA (e-mail: ylu8@ncsu.edu; sasha@ncsu.edu).

well as its optimality under a fair time-share constraint.

The investigations [14], [15] employ idealistic assumptions, including static SUs and perfect CSI knowledge at the sensor while [16] presents a two-dimensional partially observable Markov decision process (POMDP) framework for CSI tracking assuming pedestrian speeds. We investigate vehicular CR systems where fading CSI quickly becomes outdated. To enable the proposed CSI adaptation prior to sensing, we develop a CR-specific pilot-based multipath fading prediction method and analyze its overhead requirements. Moreover, we evaluate the impact of frequency correlation on multichannel diversity provided by CSI-adaptive strategies.

Contributions:

- Provide throughput and diversity analysis of a distributed sensing strategy for a hardware-constrained CR system (first proposed in [1]) that adapts the reward to the channel gain of the SU link.
- Combine the proposed CSI-adaptive sensing policy with FCFS MAC and demonstrate significant throughput gains over nonadaptive sensing strategies.
- Demonstrate robustness of the CSI-aided sensing strategy to mobile speed, correlated fading, and pilot overhead.

The rest of this paper is organized as follows. The proposed CSI-aided sensing strategy is described in Section II. This strategy is combined with an efficient MAC method and analyzed in Section III. Section IV contains numerical performance comparison of several sensing strategies and analysis of a pilot-based CSI prediction method for mobile CR networks. Finally, Section V concludes the paper.

II. CHANNEL-ADAPTIVE MYOPIC SENSING

We consider an overlay CR ad hoc network [17] where M SU pairs seek spectrum opportunities on N non-overlapping channels in a fully distributed manner. We assume CR network traffic is backlogged initially and remains backlogged over the entire time horizon.¹ The PU traffic is modeled as a stationary Markov process [18], [19] with independently evolving channels. The transition probabilities are assumed known to all SUs. Both the primary and the CR networks share the same slotted structure and are perfectly synchronized [5].²

In a typical CR network, the transmission range of the PUs is normally much larger than that of the SUs, so we assume that for each SU pair, both the transmitter and the receiver are affected by the same set of PUs and experience the same spectrum opportunities. SUs are required to sense the spectrum before accessing any channel, and can transmit only if the channel is sensed idle. We assume each SU can sense only one channel within each time slot due to the hardware constraints.

The notation used in this paper is summarized in Table I.

To infer the current PU traffic state, each SU maintains a belief vector $\theta^m(t) = [\theta^{m1}(t), \dots, \theta^{mN}(t)]$ [5]. Consider a

TABLE I
NOTATION

Notation	Explanation
N	Number of channels.
M	Number of SU pairs.
T	Number of slots over the whole time horizon [5]. Slot duration is 1 ms.
B^n	Bandwidth of channel n .
$S^{mn}(t)$	$S^{mn}(t) \in \{0(\text{busy}), 1(\text{idle})\}$. PU traffic state on channel n for SU m at time slot t .
p_{ij}^{mn}	PU Markov chain transition probability on channel n for SU m : $p_{ij}^{mn} = \Pr[S^{mn}(t)=j S^{mn}(t-1)=i]$, where $i, j \in \{0, 1\}$; assume $p_{ii}=0.8$ and $p_{ij}=0.2$, $\forall m, n$ and $i \neq j$.
$n_*^m(t)$	$n_*^m(t) \in \{1, \dots, N\}$. Sensing decision of SU m at time slot t .
$a^m(t)$	Sensing result of SU m at time slot t : $a^m(t)=1$ if the channel is sensed idle and $a^m(t)=0$ otherwise.
$\theta^{mn}(t)$	Belief probability $\theta^{mn}(t) = \Pr[S^{mn}(t)=1 n_*^m(1), a^m(1), \dots, n_*^m(t-1), a^m(t-1)]$, i.e., the conditional probability of channel n being available for SU m given past observations.
$\gamma^{mn}(t), \bar{\gamma}^{mn}$	Received instantaneous and average SNR for SU m on channel n .
$R^{mn}(t)$	Reward for SU m sensing channel n at time slot t .
$H^{mn}(\gamma^{mn}(t))$	Expected achievable throughput of SU m for sensing channel n at time slot t .
H_π^m, H_π	Average expected individual and normalized network throughputs for sensing policy π .

myopic, or greedy, sensing policy in [5]. At the first time slot $t = 1$, the initial belief vector is given by the stationary probabilities of the Markov process. Then for each $t > 1$, SU m chooses to sense the channel $n_*^m(t)$ by maximizing the expected reward $\mathbb{E}[R^{mn}(t)]$:

$$n_*^m(t) = \arg \max_n \theta^{mn}(t) R^{mn}(t). \quad (1)$$

Assuming perfect spectrum detection, the belief vector is updated as [5]:

$$\theta_r^{mn}(t) = \begin{cases} a^m(t), & \text{if } n_*^m(t) = n \\ \theta^{mn}(t), & \text{if } n_*^m(t) \neq n \end{cases} \quad (2)$$

$$\theta^{mn}(t+1) = p_{11}^{mn} \theta_r^{mn}(t) + p_{01}^{mn} (1 - \theta_r^{mn}(t)). \quad (3)$$

The process is repeated over the time horizon $t \in [1, T]$.

The myopic policy in [5] has good performance for a single SU pair scenario. However, it ignores competing SUs, and its performance degrades when multiple SUs in the neighborhood are active; since the belief vectors $\theta^m(t)$ of these SUs converge to similar values as t increases. One reason why the myopic policy is degraded in traffic-congested scenarios is the conventional reward choice given by the channel bandwidth

$$R_{\text{conv}}^{mn}(t) = B^n \quad (4)$$

which results in similar sensing decisions for all SUs. For example, when all channels have the same bandwidth (often normalized to 1), all SUs sense the most likely channel to be idle in the current time slot. This results in congestion and poor throughput. Moreover, when SUs compete for the same channel, they leave other channels unexploited, thus degrading the network throughput. Most randomized strategies in the

¹The routing and connection-level scheduling of SU traffic for minimizing the queueing delay is beyond our scope.

²Even if the PU traffic is unslotted, i.e., continuous, it can be converted into an equivalent slotted traffic model with certain collision constraints [20]. In practice, perfect synchronization may be hard to achieve and PU activity state might change during SU transmission [21]. This problem can be partially corrected by using short SU packets [22] and/or in-band sensing [21].

literature [4], [6]–[10] also employ the reward (4), but modify the myopic channel selection (1) to diversify sensing decisions of different SUs. However, these methods compromise SUs' chances to sense their favorite channels.

On the other hand, we *propose to adapt the reward to the power of the link between the transmitting and receiving secondary network nodes*. Consider the m th SU transmitter-receiver pair. At time slot t , the received signal-to-noise ratio (SNR) of the link between these two SUs on the n th channel is given by $\gamma^{mn}(t) = |g^{mn}(t)|^2 P / (N_0 B^n)$ as illustrated in Fig. 1, where $g^{mn}(t)$ is the complex-valued received channel gain (the CSI), P is the transmission power, and N_0 is the power spectral density of complex additive white Gaussian noise. Suppose $\gamma^{mn}(t)$ is perfectly known at the m th SU transmitter and is fixed for the slot duration. In the proposed CSI-aided policy, the reward is given by the channel capacity

$$R_{\text{cap}}^{mn}(t) = C^{mn}(t) = B^n \log_2(1 + \gamma^{mn}(t)). \quad (5)$$

This reward is a function of the instantaneous CSI and differs among the SU pairs due to their spatial separation and channel fading. Thus, *the proposed strategy randomizes sensing decisions and improves the individual throughput*.

The reward choice (5) attempts to match the anticipated throughput prior to sensing to the actual throughput achieved if the channel is used for transmission. In this case, the expected achievable throughput is given by

$$H^{mn}(\gamma^{mn}(t)) = \theta^{mn}(t) R_{\text{cap}}^{mn}(t). \quad (6)$$

Since the rate (5) is not attainable in practice, we also investigate a realistic cross-layer design that combines CSI-aided sensing with *adaptive modulation during transmission*. For simplicity we confine our attention to continuous-rate adaptation [23] although this approach can be easily extended to discrete-rate adaptation. Assuming adaptive quadrature amplitude modulation (QAM) with fixed transmission power, we employ adaptively adjusted data rate as the reward

$$R_{\text{AM}}^{mn}(t) = B^n k^{mn}(t) \quad (7)$$

where $k^{mn}(t)$ is the maximum spectral efficiency that the system can support under a certain bit error rate (BER) constraint BER_T [23],

$$k^{mn}(t) = \log_2(1 - 1.5\gamma^{mn}(t)/\ln(5\text{BER}_T)). \quad (8)$$

In this case, the reward is matched to the expected throughput

$$H^{mn}(\gamma^{mn}(t)) = \theta^{mn}(t) R_{\text{AM}}^{mn}(t). \quad (9)$$

Note that unlike CSI-aided rewards (5) & (7), the conventional reward (4) is not matched to the expected transmission rate when channel adaptation is employed during transmission.

III. FIRST-COME-FIRST-SERVED CSI-AIDED SENSING AND ACCESS AND PERFORMANCE ANALYSIS

A. FCFS MAC

While the proposed CSI-aided strategy randomizes sensing decisions, it is still possible for several SUs to choose the same channel. However, when an idle channel is found, only one of the SUs that have participated in sensing it can transmit

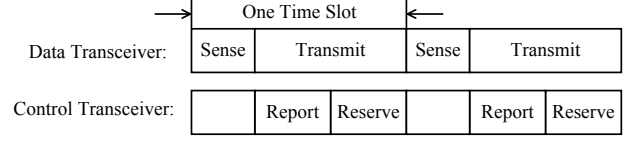


Fig. 2. Slot structure.

successfully. To avoid SU collisions, perfect *access decision resolution after sensing* has been adopted in many related references, e.g., [2], [5], [6] and is assumed in several methods evaluated in this paper.

However, in a hardware-constrained CR network, it may be desirable to avoid overlapped sensing decisions prior to sensing to prevent wasted sensing effort and to improve spectrum utilization [22]. For example, a distributed competition resolution scheme is proposed in [8] which pre-ranks the SUs and tries to evolve them onto orthogonal channels for sensing. In [9], time division fair share (TDFS) MAC is investigated, where time slots are reserved for different SUs to make individual sensing decisions in a round-robin manner from the most to the least rewarding. These two schemes are designed under the assumption that the achievable throughput on each channel is SU-invariant. However, the reward choices (5) & (7) do not satisfy this assumption. Thus the MAC methods in [8], [9] do not guarantee full contention resolution prior to sensing for CSI-aided sensing strategies and might require additional management of access requests after sensing.

To overcome this limitation, we exploit a multichannel MAC scheme based on the dynamic channel assignment (DCA) protocol [24]. DCA was intended for non-CR multichannel ad hoc networks and is often used in CR networks to resolve access requests after an available channel is found. We modified it to resolve contention prior to sensing in hardware-constrained CR networks, as illustrated in Fig. 2. Each SU is equipped with a local database and two transceivers: the control transceiver is always tuned to an out-of-band control channel [25], and the data transceiver can be tuned to any one of the N data channels. During the *reserve* phase in Fig. 2, SUs exchange control packets on the control channel prior to sensing with random backoff times to indicate the channels to be reserved for sensing according to the proposed sensing policy, as opposed to access request resolution in the original DCA MAC. SUs become aware of neighboring SUs' sensing decisions by overhearing these control messages. The current reserved channel list of all neighboring SUs is stored in the local database, which is updated when SUs learn about their neighbors' channel reservations. Unlike in DCA, reserving SUs will only transmit over the reserved channels if they are sensed idle. We assume distinct backoff time values for different SUs, resulting in perfect and sequential competition resolution on the control channel prior to sensing [25]. Moreover, low-overhead transmission of the control packets is assumed. In our proposed multichannel MAC, each channel is reserved by the first SU that requests it. Therefore, we refer this scheme as "first-come-first-served" (FCFS) MAC. Finally, we emphasize that FCFS can be easily superimposed onto almost any existing contention-based multichannel non-CR MAC, so it adds negligible overhead and energy consumption.

TABLE II
SUMMARY OF SENSING STRATEGIES

No	Strategy π	CSI-Adaptation (Y/N)	MAC (Before/After Sensing)	Expected Individual Throughput H_π^m for i.i.d. PU Traffic Model
i	Random selection	N	After	$H_{\text{Random}}^m = \sum_{n=1}^N \sum_{j=1}^M \frac{1}{j} \binom{M-1}{j-1} \left(\frac{1}{N}\right)^j \left(1 - \frac{1}{N}\right)^{M-j} \mathbb{E}[H^{mn}]$
ii	Myopic [5]	N	After	$H_{\text{My}}^m = \frac{1}{M} \mathbb{E}[H^{m1}]$
iii	Myopic with TDFS [9] ($N \geq M$)	N	Before	$H_{\text{My-TDFS}}^m = \frac{1}{M} \sum_{n=1}^M \mathbb{E}[H^{mn}] \geq H_{\text{My}}^m$
iv	Myopic with FCFS	N	Before	$H_{\text{My-FCFS}}^m = H_{\text{My-TDFS}}^m$
v	Randomized [6]	N	After	$H_{\text{Randomized}}^m = \sum_{n=1}^N \sum_{j=1}^M \frac{1}{j} \binom{M-1}{j-1} \left(\frac{\beta^n}{\sum_k \beta^k}\right)^j \left(1 - \frac{\beta^n}{\sum_k \beta^k}\right)^{M-j} \mathbb{E}[H^{mn}]$
vi	CSI-aided myopic (Section II)	Y	After	$H_{\text{CSI}}^m = \sum_{n=1}^N \sum_{j=1}^M \frac{1}{j} \binom{M-1}{j-1} (q_n)^j (1-q_n)^{M-j} \mathbb{E}[\max\{H^{m1}, \dots, H^{mN}\}]$

B. Analytical Results for Independent and Identically Distributed (i.i.d.) PU Traffic

Next, we compare several sensing strategies analytically in Table II. Assume B^n equals 1 Hz, the i.i.d. traffic model [8], [9], and perfect CSI knowledge prior to sensing. All SUs are subject to the same set of PUs and thus experience the same channel availabilities, which reduces the PU state $S^{mn}(t)$ to $S^n(t)$. The PU traffic on each channel evolves as an i.i.d. Bernoulli process with known availability probability $\beta^n = \Pr[S^n = 1], \forall n$ (omitting the time index t). First, we assume heterogeneous PU traffic statistics. Without loss of generality, let $\beta^1 > \dots > \beta^N$. Since the PU traffic exhibits no time correlation in this case, the belief probability of each SU is set equal to the channel availability probability, i.e., $\theta^{mn}(t) = \beta^n$.

We assume that all SU pairs *achieve their channel capacity with perfect CSI feedback during transmission*. Thus, when an SU m chooses channel n , the expected throughput $H^{mn}(\gamma^{mn}(t)) = \beta^n \log_2(1 + \gamma^{mn}(t))$ for all m, n (or simply H^{mn} whenever the context is clear). For sensing strategy π , the average expected individual throughput of SU m and the normalized network throughput are defined as

$$H_\pi^m \triangleq \sum_{n=1}^N \sum_{j=1}^M \frac{1}{j} \Pr[n_*^m = n, J_n^m = j-1] \cdot \mathbb{E}[H^{mn} | n_*^m = n, J_n^m = j-1]. \quad (10)$$

and

$$H_\pi \triangleq \frac{1}{M} \sum_{m=1}^M H_\pi^m \quad (11)$$

respectively, where J_n^m is the number of SUs sensing channel n excluding SU m , the channel n_*^m is selected according to the sensing strategy π , the expectation in (10) is over the channel SNR $\gamma^{mn}(t)$, and the $\frac{1}{j}$ factor is justified by the assumption of perfect access request resolution in Section III-A. Assuming i.i.d. Rayleigh fading over all channels and SU links with the average SNR $\bar{\gamma}^{mn} = \bar{\gamma}$, the cumulative distribution function

(CDF) of H^{mn} is given by [26]

$$F_{H^{mn}}(x) = 1 - \exp\left(-\frac{1}{\bar{\gamma}} \left(2^{x/\beta^n} - 1\right)\right). \quad (12)$$

The six sensing strategies in Table II are classified by their rewards and MAC methods. Strategies (i-v) do not adapt to CSI prior to sensing and employ the conventional bandwidth reward (4) although they utilize adaptive transmission after sensing. Note that the expected value $\mathbb{E}[H^{mn}] = \int_0^\infty [1 - F_{H^{mn}}(x)] dx$. On the other hand, the proposed strategy (vi) is CSI-adaptive prior to sensing, and the reward (5) is matched to the expected achievable throughput (6). We provide a proof for H_{CSI}^m in the Appendix. The probability

$$q_n \triangleq \Pr[n_*^m = n] = \Pr[\arg \max_n H^{mn} = n] \quad (13)$$

and

$$\mathbb{E}[\max\{H^{m1}, \dots, H^{mN}\}] = \int_0^\infty \left[1 - \prod_{n=1}^N F_{H^{mn}}(x)\right] dx. \quad (14)$$

Other formulas in Table II are proved similarly [26].

We also derived in [26] the average expected individual throughputs H_π^m of CSI-aided myopic sensing with TDFS and FCFS (labeled as policies vii & viii, respectively) as well as that of the centralized sum-rate optimal policy (ix) assuming $M=N=2$. In the sum-rate optimal policy (ix), the SUs are coordinated by a central controller (e.g., an access point or a base station), and the throughput of this policy provides an upper bound on the throughputs of the distributed policies (i-viii). The three policies (vii-ix) employ CSI-adaptation and contention resolution prior to sensing. We were not able to obtain the throughput expressions of these policies for arbitrary $N, M \geq 2$.

Assuming $M=N=2$ and $\beta^2 = 0.4$, the normalized network throughputs (11) are compared as a function of β^1 in Fig. 3. First, we compare performance of the policies that employ contention resolution after sensing. Note that the myopic policy (ii) performs even worse than the naïve random channel selection approach (i) since in the former both SUs favor

channel 1 and always compete to gain access, leaving channel 2 unexploited. The randomized sensing policy (v) reduces overlapped sensing decisions, but it reduces the SUs' chances of sensing their favorite channels and sacrifices the individual throughput to compensate for possible SU collisions, so has small performance gain over the random selection approach (i). The proposed CSI-aided myopic sensing policy (vi) achieves better performance than the policies above.

Next, we consider MAC prior to sensing. When applied to the myopic policy, the proposed FCFS scheme (Section III-A) and the TDFS scheme [9] achieve identical throughputs and on average provide equal share of spectrum opportunities to the two SUs (iii & iv). On the other hand, when applied to the CSI-aided myopic policy, TDFS (vii) actually degrades performance while FCFS (viii) results in significant improvement. FCFS can still identify overlapped SU sensing decisions through control message exchange in this case, while TDFS requires SUs to cede its preferred channel to the other SU for half of the time to combat anticipated SU competition. However, in CSI-aided sensing strategies, the channel preference depends on the local CSI of each SU. Thus, the nonpreferred channel of the ceding SU can be the preferred channel of the other SU, resulting in conflicted sensing decision. Therefore, TDFS undermines the randomizing effect of CSI-aided sensing and reduces its throughput.

Note also that while the centralized policy (ix) outperforms the CSI-aided myopic policy with FCFS (viii), the latter is more fair since it provides SUs with the opportunity to sense their preferred channels at any time with equal probabilities while in (ix) these chances are compromised to achieve the optimal sum-rate. We found that numerical results for i.i.d. PU traffic and larger N, M values do not provide additional insights [26].

Finally, we quantify the benefits of multiuser and multi-channel diversity for the proposed CSI-aided sensing policy in Section II assuming a homogeneous environment where all Rayleigh fading channels are i.i.d. with the average SNR $\bar{\gamma}^{mn} = \bar{\gamma}$ and the PU traffic follows i.i.d. Bernoulli process with $\beta^n = \beta$.³ From [26],

$$H_{\text{CSI}}^m = \mathbb{E} [\max\{H^{m1}, \dots, H^{mN}\}] g^{MN} \quad (15)$$

where the expectation is given by (14) and

$$g^{MN} \triangleq N \sum_{j=1}^M \frac{1}{j} \binom{M-1}{j-1} \left(\frac{1}{N}\right)^j \left(1 - \frac{1}{N}\right)^{M-j} \quad (16)$$

quantifies each SU's share of spectrum opportunities in a multi-SU setting. The expression in (15) balances the multi-channel diversity gain vs. SU competition tradeoff. For example, when $M = N$, (16) reduces to $g^{MM} = 1 - (1 - \frac{1}{M})^M$, which decreases with M [26], thus indicating more intense SU competition for larger M . On the other hand, the expectation in (15) corresponds to selection combining (SC) diversity

³Note that it is generally difficult to analyze diversity systems in closed-form for a heterogeneous environment, and thus identical statistics for all diversity branches are often assumed in the study of diversity combining, e.g., [27]. Moreover, the homogeneous assumption is useful when the CR network is not yet or being constructed because SUs may not have sufficient knowledge of the PU traffic or fading statistics at that time.

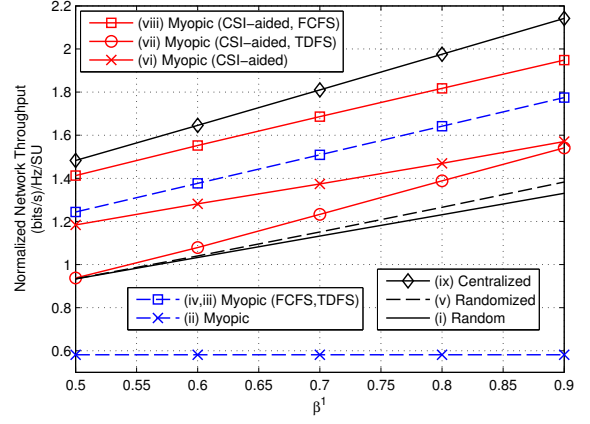


Fig. 3. Analytical throughput vs. β^1 ; $\beta^2=0.4$; capacity reward; 2 SU pairs; 2 channels; i.i.d. Rayleigh fading; average SNR=10 dB.

gain [27], which increases with M . Note that (15) provides guidelines for CR network design. For example, if the SU network capacity (M) is fixed, the number of channels (N) can be optimized using (15) exploiting the tradeoff between SC diversity gain (which saturates for large M) and the cost of network setup or channel leasing [2]. Similarly, for fixed N , the optimal M can be determined based on (15) to prevent extremely high SU competition.

IV. NUMERICAL SIMULATION RESULTS

In Sections IV-A and IV-B, we present simulation results for a network with $M = 3$ SUs and $N = 10$ channels. It represents a small hardware-constrained network, for example, a sparse rural CR network. However, small network size does not preclude SU competition since the number of available channels is also small. In Section IV-C, we investigate performance trends for varying M and N parameters.

We assume *independent Rayleigh fading* for all SU pairs and channels with average SNR=10 dB unless stated otherwise. The instantaneous SNR $\gamma^{mn}(t)$ is fixed over the duration of one time slot (1 ms). A Markovian PU traffic model is employed (see Table I).

A. Performance Comparison for Ideal CSI

In Fig. 4, the throughputs of policies (i-viii) in Section III-B and the modified myopic policy with collision avoidance (myopic/CA) [7] are compared over the time interval of 20 ms. In the latter strategy, each SU maintains a variable-length list of candidate channels based on the past history of MAC-layer SU collisions (or conflicting sensing decisions) and uniformly selects one channel on the list for sensing at each time slot. We assume perfect CSI knowledge at the sensor and ideal spectrum sensing. The maximum Doppler shift f_{dm} is 40 Hz although the performance is not sensitive to f_{dm} under the perfect CSI assumption.

Note that the throughputs of all strategies approach their asymptotic values as time increases. The sensing history and the belief vectors (2)-(3) of different SUs differ slightly in the Fig. 4 scenario, as SUs attempt to predict channel availabilities with partially observed PU traffic states. Thus, unlike in

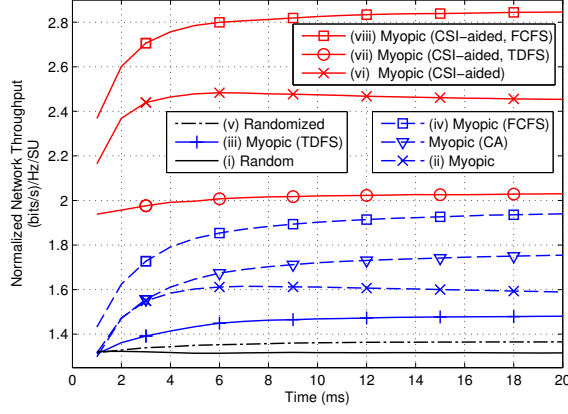


Fig. 4. Throughput vs. time; capacity reward; 3 SU pairs; 10 channels; i.i.d. Rayleigh fading; average SNR=10 dB; $f_{dm}=40$ Hz.

Fig. 3, the myopic policy (ii) provides about 0.3 (bits/s)/Hz/SU improvement over the random selection approach (i) because different SUs make similar, but not identical sensing decisions. This observation also provides insight into relatively poor performance of the myopic policy with TDFS (iii) when compared with that in Fig. 3. Note that an SU senses its favorite channel for $1/M$ of the time using TDFS MAC, so its throughput loss is exacerbated by a larger number of SUs M in Fig. 4 relative to Fig. 3.

The myopic/CA policy effectively reduces SU collisions and restores the gain obtained from PU traffic cognition. However, it acts only after SUs collide whereas the CSI-aided myopic policy (vi) takes advantage of fading variation to randomize sensing decisions and to boost the individual throughput. Due to a larger number of channels N , SUs achieve greater benefit from multichannel diversity and thus higher throughput gain of CSI-aided sensing than in Fig. 3. The gains of the CSI-aided myopic strategy (vi) over the myopic (ii) and myopic/CA strategies are about 0.9 and 0.7 (bits/s)/Hz/SU (or about 50% and 40%), respectively. An additional gain of about 0.4 (bits/s)/Hz/SU (or over 15%) can be achieved by applying the FCFS MAC with the CSI-aided strategy (viii vs. vi). We also note that FCFS offers a gain of 0.35 (bits/s)/Hz/SU (or 20%) when used with the conventional myopic strategy (iv vs. ii) and outperforms other nonadaptive strategies.

In Fig. 5, we investigate the throughput averaged over 20 slots vs. the average SNR for the sensing strategies that employ adaptive modulation during transmission. In this case, the reward for the CSI-adaptive strategies is given by (7) and the throughput during transmission is given by (9) for all strategies. We observe that the proposed CSI-aided policy (vi) outperforms the myopic policy (ii) by at least 5 dB. The gain over the myopic/CA policy [7] decreases with the average SNR, but is at least 3 dB for a practical average SNR ≤ 30 dB. Moreover, the FCFS scheme provides 2-4 dB performance gain over the CSI-aided myopic strategy (viii vs. vi) and up to 4 dB gain over the conventional myopic strategy (iv vs. ii). Similar SNR gains were observed when the adaptation is to the channel capacity [see (5)-(6)] and for the shadow fading channel model [26]. Guided by the results in Fig. 4 and Fig. 5, we consider only the CSI-adaptive and the nonadaptive myopic

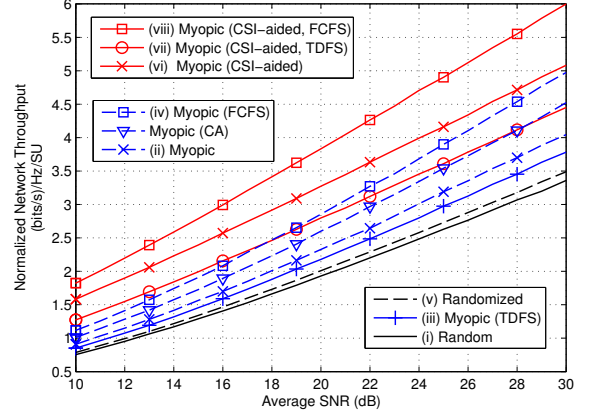


Fig. 5. Throughput vs. average SNR; continuous-rate adaptation; fixed transmission power; $\text{BER}_T=10^{-3}$; 3 SU pairs; 10 channels; i.i.d. Rayleigh fading; $T=20$ slots.

policies with/without FCFS, i.e., (ii, iv, vi, viii), in the remainder of the paper since other strategies do not significantly improve upon (ii). Also, we assume that all strategies achieve the expected throughput (6) and all CSI-aided policies use the capacity reward (5).

Finally, the throughput of the proposed CSI-aided strategies with imperfect sensing was analyzed in [1], [26] for moderate received PU signal strength. It was shown that the proposed CSI-aided strategy maintains about 0.8 (bit/s)/Hz/SU gain over the conventional myopic strategy while the FCFS MAC provides an extra gain of over 0.3 (bits/s)/Hz/SU when the target miss detection probability is greater or equal to 0.1. Moreover, in [28], combined adaptive threshold control and channel-aware sensing strategies were proposed to improve the sensing quality and the SU throughput for very low PU signal SNR.

B. Adaptation to Multipath Fading CSI

The proposed sensing strategy relies on accurate prediction of the fading SNR $\gamma^{mn}(t)$ for the upcoming time slot prior to sensing. Such prediction is particularly challenging for CR systems since the signals of each SU transmitter-receiver pair are not confined to predefined frequency bands or time slots. Thus, it is important to ensure that the proposed policies are robust to *CSI mismatch*. In this section, we explore adaptation to a short-term, or multipath, fading component of SNR $\gamma^{mn}(t)$. In [1], we investigated theoretical minimum mean square error (MMSE) fading prediction performance for the CSI-aided myopic strategy (vi) and demonstrated that it is robust to CSI errors and that its throughput degrades gracefully to that of its nonadaptive counterpart (ii) when CSI becomes unreliable. Below, we propose and evaluate a realistic fading prediction method customized to CR networks.

In conventional wireless communication systems, fading CSI can be predicted using previously received pilot signals [29], [30]. However, in CR, SUs can send pilots only on channels that are free of PU transmissions. We propose the following pilot placement method to aid CSI prediction prior to sensing. In this method, all SUs report their sensing results using a control channel as in the *reporting* phase of [31, Fig. 3-4] at the beginning of each time slot after spectrum sensing

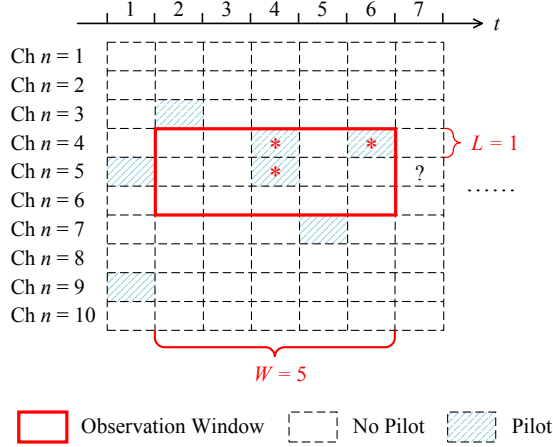


Fig. 6. Observation window of SU m for predicting $\gamma^{m,5}(7)$ (marked “?”).

(cf. Fig. 2). Thus, SUs learn which channels are idle in the current time slot. Note that exchange of CSI is not required for the proposed method. Each SU receiver sends pilots on the idle channels discovered by itself and its neighbors. When a pilot is sent by the receiver of the m th SU pair over channel n at time slot t , the m th SU sensor (transmitter) obtains a noisy observation of the complex-valued channel gain $g^{mn}(t)$ by reciprocity (Fig. 1). To predict the channel coefficient $\hat{g}^{mn}(t)$, SU transmitter m collects all such received noisy pilots on the n th channel and its adjacent channels within a time window $\{t - W, \dots, t - 1\}$ and a frequency window of width $2L + 1$ centered at channel n . For example, consider the pilot transmission pattern in Fig. 6. To obtain the predicted channel coefficient at $t = 7$ on the fifth channel, or $\hat{g}^{m,5}(7)$ (marked as “?” in Fig. 6), SU transmitter m extracts the CSI from the received pilots within the observation window shown by the solid rectangular box with $W = 5$ and $L = 1$ in Fig. 6. The collected pilots’ locations are marked with “*” in Fig. 6. Then, the MMSE long range prediction algorithm [30] is used to calculate the predicted channel coefficient and the expected reward [10, eq. (7)] at the beginning of each time slot based on the observations of these pilots. The complexity of this method is on the order of $\mathcal{O}(p^{mn}(t)^3)$, where $p^{mn}(t)$ is the number of pilots falling into the observation window [26].

We assume a known channel autocorrelation matrix. In practice, adaptive prediction methods can be used to track fading parameter variation [29]. We employ the ETSI Vehicular-A channel [32] which has six paths and an rms delay of 633 ns. Each channel is subject to frequency-flat fading. The time-varying channel coefficients are generated independently on each path and for each SU pair using the deterministic modified Jakes model [33], and thus we consider a longer time horizon of $T = 10^5$. Perfect pilot transmission scheduling among the SUs and negligible pilot overhead are assumed. In Fig. 7, the throughputs of the CSI-aided sensing policies (vi,viii) and the normalized mean square errors (NMSEs) of CSI prediction (averaged over the whole time horizon and all SUs) are compared as a function of f_{dm} for $B^n = 200$ kHz. We observe that the averaged NMSEs in Fig. 7(b) grow with f_{dm} (or the mobile speed), thus degrading the throughputs of the CSI-aided myopic sensing policies in Fig. 7(a). As f_{dm}

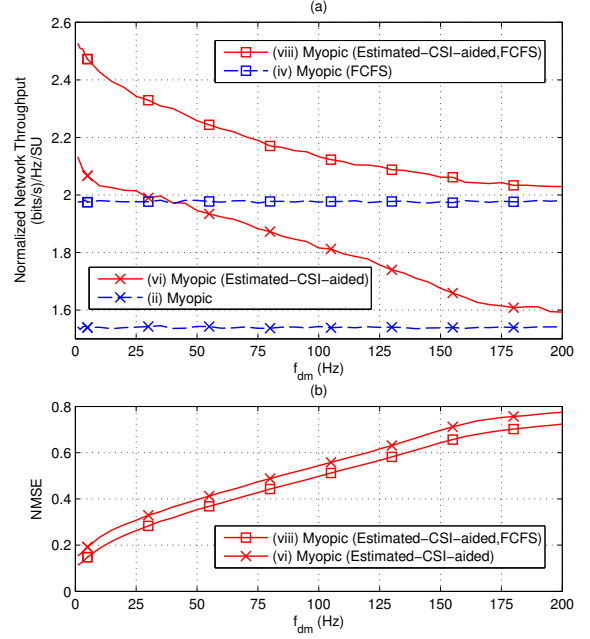


Fig. 7. Performance of CSI-adaptive strategies with predicted CSI vs. f_{dm} : (a) throughput comparison with nonadaptive strategies (b) prediction NMSE; 3 SU pairs; 10 channels; ETSI Vehicular-A channel model; average SNR= 10 dB; $B^n=200$ kHz; $L=1$; $W=20$; $T=10^5$ slots.

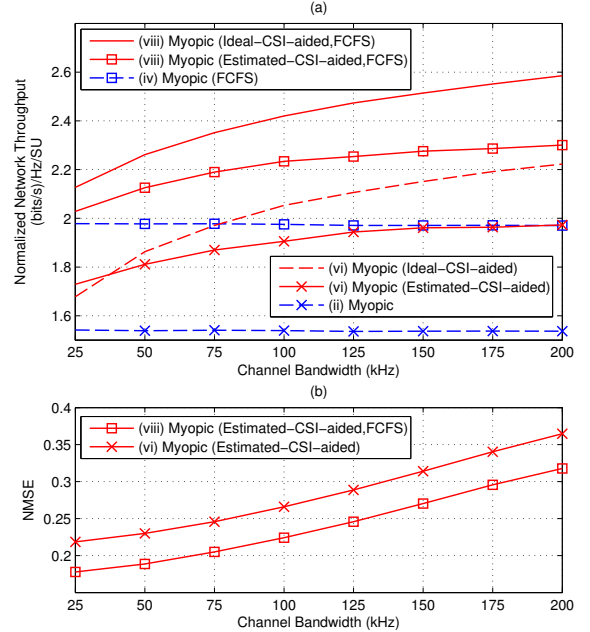


Fig. 8. Performance of CSI-adaptive strategies with predicted CSI vs. channel bandwidth: (a) throughput of adaptive and nonadaptive policies (b) prediction NMSE; 3 SU pairs; 10 channels; ETSI Vehicular-A channel model; average SNR= 10 dB; $f_{dm}=40$ Hz; $L=1$; $W=20$; $T=10^5$ slots.

approaches 200 Hz, the latter converge to their nonadaptive counterparts (ii,iv), respectively. The FCFS MAC completely eliminates overlapped sensing decisions so SUs can potentially discover additional idle channels for pilot transmissions. Thus, the FCFS MAC improves CSI estimation accuracy (see Fig. 7(b)) and provides an additional throughput gain of about 0.4 (bits/s)/Hz/SU over the CSI-aided myopic sensing policy alone for mismatched CSI (viii vs. vi) in Fig. 7(a).

In Fig. 8, we compare these policies as a function of the

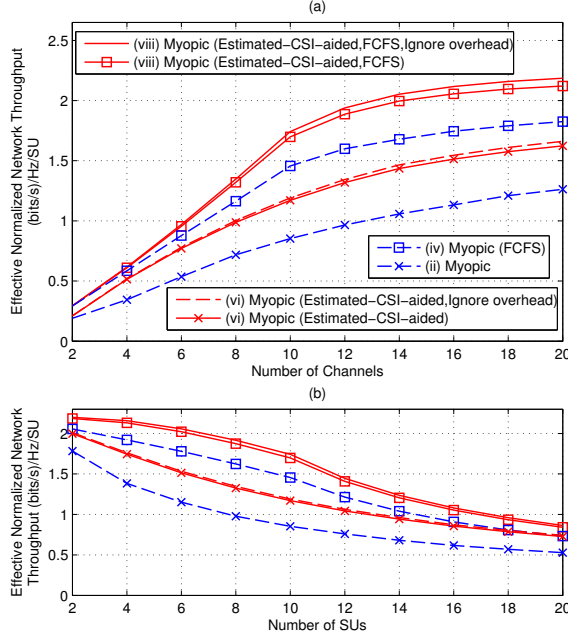


Fig. 9. Performance of CSI-adaptive strategies with pilot overhead: (a) varying N with $M = 10$; (b) varying M with $N = 10$; ETSI Vehicular-A channel model; average SNR = 10 dB; $f_{dm} = 75$ Hz; $B^n = 200$ kHz; $L = 1$; $W = 20$; $T = 10^3$ slots.

channel bandwidth for $f_{dm} = 40$ Hz. We first note from Fig. 8(b) that the predicted CSI is more accurate for smaller channel bandwidths since frequency correlation between future channel gains and past observations collected from adjacent channels decreases with channel bandwidth. Thus, for CSI-aided sensing policies (vi, viii), the gap between the throughput curves for ideal and mismatched CSI widens as the bandwidth increases in Fig. 8(a). However, better CSI prediction does not lead to improved throughput in Fig. 8(a). This seemingly conflicting result is mainly due to the tradeoff between the CSI prediction accuracy and multichannel diversity. As the channel bandwidth grows, the correlation between the channels decreases, and the throughput gain of CSI-adaptation increases, compensating for decreased prediction accuracy. Overall, our proposed CSI-adaptive sensing policies (vi, viii) outperform their nonadaptive counterparts (ii, iv) for $f_{dm} \leq 200$ Hz and $B^n \in [25, 200]$ kHz for the Vehicular-A channel model. The gain is on the order of 0.4 (bits/s)/Hz/SU for typical system parameters and modest mobile speed, i.e., for $B^n \geq 75$ kHz and $f_{dm} \leq 75$ Hz (or when the carrier frequency ≤ 1 GHz and the mobile speed ≤ 50 mph [29]).

C. Effects of System Parameters and Pilot Overhead

We vary the number of channels (N) and SUs (M) in Fig. 9(a) and Fig. 9(b), respectively. Note that the SU throughput increases with the amount of spectrum resources (N) and decreases with the number of competitors (M). Moreover, Fig. 9 shows the effect of pilot overhead. In the proposed method, each SU sends one pilot symbol per slot in each channel that was sensed to be idle. The symbol interval $T_{sym} = 1/B^n = 5 \mu s$. At each time slot t , the total number of pilot transmissions in the CR system is $N_p(t) \times M$, and the total number of transmitted symbols is $N_p(t) \times 1 \text{ ms}/T_{sym}$,

where $N_p(t)$ is the number of sensed available channels. Thus, the results in Fig. 9 show very negligible pilot overhead since $M \in [2, 20]$ is much smaller than $1 \text{ ms}/T_{sym} = 200$.

In practice, pilot overhead increases with M , mobile speed, and reduced number of symbols per slot. To compensate, the proposed method can be enhanced by low-power pilot signals transmitted under the noise level of the PU network during the busy slots [34] or by channel gain estimation in the presence of sensing errors [35]. Moreover, each SU can reduce its pilot rate or choose only a subset of channels for CSI tracking since multichannel diversity saturates as the number of diversity branches increases [27]. Finally, in case of bursty SU traffic, SUs can transmit pilots only when they have data to transmit or shortly before transmission to reduce pilot overhead. On the other hand, high PU activity, low channel correlation, or hardware constraints result in insufficient pilot availability and limit prediction accuracy. If prediction of the multipath fading component becomes infeasible due to fast mobile speed (Fig. 7), the proposed strategies can adapt to slowly varying long-term (shadow) fading CSI. Using statistical and realistic physical shadow fading channel models, we demonstrated in [1], [26], [28] that CSI-aided strategies retain significant gains over conventional sensing policies and are robust to spatial and frequency correlation in CR ad hoc networks.

V. CONCLUSION

A channel-aware sensing strategy was investigated for distributed hardware-constrained mobile CR networks. To achieve effective collision resolution, this strategy was combined with a novel multichannel FCFS MAC algorithm. Analysis and simulations showed that adaptation to the CSI of the secondary link prior to sensing randomizes sensing decisions and improves both the individual and network throughputs. The throughput and energy gains of the proposed CSI-aided myopic strategy were on the order of 40% and 3 dB, respectively, relative to sensing policies in the literature. Moreover, combining this strategy with FCFS MAC provided additional gains of approximately 15% and 2-4 dB, respectively. Finally, a pilot-based fading prediction method was developed to enable CSI-aided sensing strategies, and it was demonstrated that the proposed sensing strategies are robust to CSI mismatch and frequency correlation in practical mobile CR ad hoc networks.

APPENDIX A

PROOF OF THROUGHPUT FORMULA FOR (VI) IN TABLE II

As the sensing decisions are made individually without negotiating before sensing, the following properties hold $\forall m, n$:

$$\Pr[n_*^m = n, J_n^m = j-1] = \Pr[n_*^m = n] \Pr[J_n^m = j-1] \quad (17)$$

$$\mathbb{E}[H^{mn} | n_*^m = n, J_n^m = j-1] = \mathbb{E}[H^{mn} | n_*^m = n]. \quad (18)$$

The sensing decisions are made by (1) with the reward (5). Assuming $\theta^{mn}(t) = \beta^n$, $\forall m, n$, the sensing policy becomes

$$n_*^m = \arg \max_n H^{mn}, \quad (19)$$

which follows from the definition of H^{mn} (6) and

$$\Pr[J_n^m = j-1] = \binom{M-1}{j-1} (q_n)^{j-1} (1-q_n)^{M-j} \quad (20)$$

for all m, n and $j \leq M$, where q_n (13) has the same value for all m because both the channel availability β^n and the average SNR $\bar{\gamma}^{mn} = \bar{\gamma}$ are SU-invariant. Using (17)-(18) in (10) and from (19)-(20), we obtain H_{CSI}^m in Table II.

REFERENCES

- [1] Y. Lu and A. Duel-Hallen, "Channel-adaptive sensing strategy for cognitive radio ad hoc networks," in *Proc. IEEE CCNC'13*, 2013, pp. 466–471.
- [2] J. Jia, Q. Zhang, and X. Shen, "HC-MAC: A hardware-constrained cognitive MAC for efficient spectrum management," *IEEE J. Sel. Areas Commun.*, vol. 26, no. 1, pp. 106–117, 2008.
- [3] I. F. Akyildiz, W. Y. Lee, and K. R. Chowdhury, "CRAHNS: Cognitive radio ad hoc networks," *Ad Hoc Netw.*, vol. 7, no. 5, pp. 810–836, 2009.
- [4] L. Lai, H. E. Gamal, H. Jiang, and H. V. Poor, "Cognitive medium access: Exploration, exploitation, and competition," *IEEE Trans. Mobile Comput.*, vol. 10, no. 2, pp. 239–253, 2011.
- [5] Q. Zhao, L. Tong, A. Swami, and Y. Chen, "Decentralized cognitive MAC for opportunistic spectrum access in ad hoc networks: A POMDP framework," *IEEE J. Sel. Areas Commun.*, vol. 25, no. 3, pp. 589–600, 2007.
- [6] K. Liu, Q. Zhao, and Y. Chen, "Distributed sensing and access in cognitive radio networks," in *Proc. IEEE ISSSTA'08*, 2008, pp. 23–27.
- [7] Y. Lee, "Modified myopic policy with collision avoidance for opportunistic spectrum access," *Electron. Lett.*, vol. 46, no. 12, pp. 871–872, 2010.
- [8] A. Anandkumar, N. Michael, A. K. Tang, and A. Swami, "Distributed algorithms for learning and cognitive medium access with logarithmic regret," *IEEE J. Sel. Areas Commun.*, vol. 29, no. 4, pp. 731–745, 2011.
- [9] K. Liu and Q. Zhao, "Distributed learning in multi-armed bandit with multiple players," *IEEE Trans. Signal Process.*, vol. 58, no. 11, pp. 5667–5681, 2010.
- [10] Y. Xu, J. Wang, Q. Wu, A. Anpalagan, and Y. D. Yao, "Opportunistic spectrum access in unknown dynamic environment: A game-theoretic stochastic learning solution," *IEEE Trans. Wireless Commun.*, vol. 11, no. 4, pp. 1380–1391, 2012.
- [11] V. Asghari and S. Aissa, "Adaptive rate and power transmission in spectrum-sharing systems," *IEEE Trans. Wireless Commun.*, vol. 9, no. 10, pp. 3272–3280, 2010.
- [12] A. Bagayoko, I. Fijalkow, and P. Tortelier, "Power control of spectrum-sharing in fading environment with partial channel state information," *IEEE Trans. Signal Process.*, vol. 59, no. 5, pp. 2244–2256, 2011.
- [13] A. W. Min and K. G. Shin, "Exploiting multi-channel diversity in spectrum-agile networks," in *Proc. IEEE INFOCOM'08*, 2008, pp. 1921–1929.
- [14] H. T. Cheng and W. Zhuang, "Simple channel sensing order in cognitive radio networks," *IEEE J. Sel. Areas Commun.*, vol. 29, no. 4, pp. 676–688, 2011.
- [15] J. Zhao and X. Wang, "Channel sensing order in multi-user cognitive radio networks," in *Proc. IEEE DySPAN'12*, 2012, pp. 397–407.
- [16] Y. Wang, Y. Xu, L. Shen, C. Xu, and Y. Cheng, "Two-dimensional POMDP-based opportunistic spectrum access in time-varying environment with fading channels," *J. Commun. Netw.*, vol. 16, no. 2, pp. 217–226, 2014.
- [17] Q. Zhao and B. M. Sadler, "A survey of dynamic spectrum access," *IEEE Signal Process. Mag.*, vol. 24, no. 3, pp. 79–89, 2007.
- [18] A. J. Gibson and L. Arnett, "Statistical modelling of spectrum occupancy," *Electron. Lett.*, vol. 29, no. 25, pp. 2175–2176, 1993.
- [19] S. Geirhofer, L. Tong, and B. M. Sadler, "Cognitive radios for dynamic spectrum access-dynamic spectrum access in the time domain: Modeling and exploiting white space," *IEEE Commun. Mag.*, vol. 45, no. 5, pp. 66–72, 2007.
- [20] Y. Xu, A. Anpalagan, Q. Wu, L. Shen, Z. Gao, and J. Wang, "Decision-theoretic distributed channel selection for opportunistic spectrum access: Strategies, challenges and solutions," *IEEE Commun. Surveys Tuts.*, vol. 15, no. 4, pp. 1689–1713, 2013.
- [21] C. Zhang and K. G. Shin, "What should secondary users do upon incumbents' return?" *IEEE J. Sel. Areas Commun.*, vol. 31, no. 3, pp. 417–428, 2013.
- [22] X. Zhou, G. Y. Li, Y. H. Kwon, and A. C. K. Soong, "Detection timing and channel selection for periodic spectrum sensing in cognitive radio," in *Proc. IEEE GLOBECOM'08*, 2008, pp. 1–5.
- [23] S. T. Chung and A. J. Goldsmith, "Degrees of freedom in adaptive modulation: A unified view," *IEEE Trans. Commun.*, vol. 49, no. 9, pp. 1561–1571, 2001.
- [24] J. Mo, H. S. W. So, and J. Walrand, "Comparison of multichannel MAC protocols," *IEEE Trans. Mobile Comput.*, vol. 7, no. 1, pp. 50–65, 2008.
- [25] B. F. Lo, "A survey of common control channel design in cognitive radio networks," *Physical Commun.*, vol. 4, no. 1, pp. 26–39, 2011.
- [26] Y. Lu, "CSI-adaptive spectrum detection, sensing, and access for cognitive radio ad hoc networks," Ph.D. dissertation, North Carolina State Univ., in preparation, 2015.
- [27] D. G. Brennan, "Linear diversity combining techniques," *Proc. IEEE*, vol. 91, no. 2, pp. 331–356, 2003.
- [28] Y. Lu and A. Duel-Hallen, "Channel-adaptive spectrum detection and sensing strategy for cognitive radio ad-hoc networks," in *Proc. 51st Allerton Conf. Commun., Control, Comput.*, 2013, pp. 1408–1414.
- [29] A. Duel-Hallen, "Fading channel prediction for mobile radio adaptive transmission systems," *Proc. IEEE*, vol. 95, no. 12, pp. 2299–2313, 2007.
- [30] L. Ming, A. Duel-Hallen, and H. Hallen, "Reliable adaptive modulation and interference mitigation for mobile radio slow frequency hopping channels," *IEEE Trans. Commun.*, vol. 56, no. 3, pp. 352–355, 2008.
- [31] H. Su and X. Zhang, "Cross-layer based opportunistic MAC protocols for QoS provisionings over cognitive radio wireless networks," *IEEE J. Sel. Areas Commun.*, vol. 26, no. 1, pp. 118–129, 2008.
- [32] *Universal Mobile Telecommunications System (UMTS); Selection procedures for the choice of radio transmission technologies of the UMTS*, ETSI Std. TR 101 112 V3.1.0, 1997.
- [33] P. Dent, G. E. Bottomley, and T. Croft, "Jakes fading model revisited," *Electron. Lett.*, vol. 29, no. 13, pp. 1162–1163, 1993.
- [34] A. Tajer and X. Wang, "Beacon-assisted spectrum access with cooperative cognitive transmitter and receiver," *IEEE Trans. Mobile Comput.*, vol. 9, no. 1, pp. 112–126, 2010.
- [35] M. C. Gursoy and S. Gezici, "On the interplay between channel sensing and estimation in cognitive radio systems," in *Proc. IEEE GLOBECOM'11*, 2011, pp. 1–5.



Yuan Lu received her B.E. degree in electrical engineering from Southeast University, Nanjing, China, in 2008. Since 2009, she has been working towards the Ph.D. degree in the Department of Electrical and Computer Engineering at North Carolina State University, Raleigh, NC. Her research interests are in the areas of cognitive radio, wireless and digital communications, signal detection and estimation, cross-layer design, and cooperative game theory.



Alexandra Duel-Hallen received her Ph.D. in electrical engineering from Cornell University in 1987. During 1987–1990, she was a Visiting Assistant Professor at the School of Electrical Engineering, Cornell University, Ithaca, NY. In 1990–1992, she was with the Mathematical Sciences Research Center, AT&T Bell Laboratories, Murray Hill, NJ. She joined the Electrical and Computer Engineering Department at North Carolina State University in 1993. From 1990 to 1996, Dr. Duel-Hallen was an Associate Editor for the IEEE Transactions on Communications. In 2000–2002, she served as a Guest Editor for two Special Issues on Multiuser Detection for the IEEE Journal on Selected Areas in Communications. She is listed in American Men and Women in Science published by Cengage Learning and in Thomson Reuters Highly Cited Research, <http://researchanalytics.thomsonreuters.com/highlycited/>. Her paper was included in The Best of the Best: Fifty Years of Communications and Networking Research (56 papers in Communications and Networking), IEEE Press, 2007, and the IEEE Communications Society 50th Anniversary Journal Collection as one of 41 key papers in physical and link layer areas, 1952–2002. She is a Fellow of the IEEE. Dr. Duel-Hallen's current research interests are in wireless communications and networking for power systems.